Available online at www.sciencedirect.com
ScienceDirect
Cement & Concrete Composites 30 (2008) 854–860
Cement & Concrete Composites
www.elsevier.com/locate/cemconcomp

Behavior of air-entrained concrete under the compression with constant confined stress after freeze–thaw cycles

Shang Huai-shuai [a,b,*], Song Yu-pu [a]

[a] Dalian University of Technology, Dalian 116024, China
[b] Shandong Provincial Academy of Building Research, Jinan 250031, China

Received 21 June 2006; received in revised form 18 October 2007; accepted 22 October 2007
Available online 5 November 2007

Abstract

Properties of air-entrained concrete under compressive loads with constant confined stress after 0, 100, 200, 300 and 400 cycles of freeze–thaw were studied. The failure characteristic of specimens and the direction of the crack are observed. Based on the test data, the influence of freeze–thaw cycles and lateral compressive stress ratio on the ultimate compressive strength is analyzed, respectively. The relationships between the ultimate compressive strength and freeze–thaw cycles, lateral compressive stress ratio are given, respectively. The unified failure criterion with consideration of the influence of freeze–thaw cycles and stress ratio is proposed. It provides the experimental and theory foundations for strength analysis of air-entrained concrete structures subject to complex loads in cold environment.

Keywords: Air-entrained concrete; Freeze–thaw cycle; Stress ratio; Strength criteria; Lateral stress

1. Introduction

The durability [1–3] problems that arise in concrete exposed to freeze–thaw cycles is of utmost importance in countries having subzero temperature conditions, such as the northern cold regions in China. In cold environments, freezing and thawing can be harmful for a porous brittle material such as concrete when it is subjected to lower temperatures. As more and more concrete structures (dams, hydraulic structures and offshore structures) are being built in harsher environments, the concrete material may deteriorate rapidly after repeated cycles of freeze–thaw. Hence, demand for durable concrete has increased. One of the greatest advances in concrete technology was the development of air-entrained concrete in the late 1930s. Today, air entrainment is recommended for nearly all concretes, principally to improve resistance to freeze–thaw cycles when exposed to water and deicing chemicals.

There is great change in the properties of concrete after freeze–thaw cycles. Jacobsen et al. [4] investigated the effect of internal cracking on ice formation for high strength concrete. Buck [5] found that freezing and thawing resistance of the concrete containing recycled concrete, where chert gravel was the original aggregate, increased in freezing and thawing tests. Sun et al. [6] investigated damage and damage resistance of high strength concrete under double damage factors: flexural load and freeze–thaw cycles. Experimental results show that the damage process is accelerated and the extent of damage increased under the simultaneous action of load and freeze–thaw cycles. Shang and Song [7] investigated the strength and deformation behavior of plain concrete under biaxial compression after 0, 25, 50, 75 cycles of freezing and thawing. The influence of freeze–thaw cycles and stress ratio on the biaxial

* Corresponding author. Address: Dalian University of Technology, Dalian 116024, China. Tel.: +86 15990900238.
E-mail address: shanghuaishuai@yahoo.com (H.-s. Shang).

0958-9465/$ - see front matter © 2007 Elsevier Ltd. All rights reserved.
doi:10.1016/j.cemconcomp.2007.10.006

Table 1
Mix proportions and major parameters of air-entrained concrete

w/c	Cement (kg/m^3)	Sand (kg/m^3)	Coarse aggregate (kg/m^3)	Water (kg/m^3)	Air-entraining agents (kg/m^3)	Compressive strength (f_c/MPa)	Air content (%)
0.4	412.67	586.83	1186	164.3	1.03	25.64	5.5–6.5

compressive strength, the strain corresponding to peak stress and the elastic modulus was also analyzed. Qin [8] investigated the strength and deformation characteristics of plain concrete under multiaxial compression after different cycles of freeze–thaw, the conclusion that the strength decreased and deformation increased as increasing the number of freeze–thaw cycles was drawn.

The research on the strength and deformation characteristics of plain concrete under biaxial and triaxial loads has been reported [7,9–12]. But stress state of the concrete material in actual structures is very complex; the distribution of stress will change after plastic deformation, the change of boundary condition, different path and history of loads, etc. Lan [13] investigated the influence of load path on the ultimate compressive strength of plain concrete under the compression with constant confined stress. It is concluded that the strains of concrete under different loading paths are considerably different. Lü [14,15] investigated the compressive deformation and strength of the concrete under different loading rates and lateral stresses, the effect of lateral stress on the deformation is obvious.

Air-entrained concrete has broad application in actual engineering, while very little work has been documented on the strength of air-entrained concrete under the compression with constant confined stress prior to or after different cycles of freeze–thaw. It is important to have a better understanding of the strength of air-entrained concrete under the compression with constant confined stress after different cycles of freeze–thaw. This paper presents experimental study of air-entrained concrete under the compression with constant confined stress after 0, 100, 200, 300, 400 cycles of freeze–thaw according to the GBJ82-85 [16].

2. Experiment

2.1. Materials and mix proportions

The cementitious materials used for this investigation are #425 Portland cement. The coarse aggregates were a crushed stone (diameter ranging from 5 mm to 10 mm). The fine aggregates were natural river sand with fineness modulus of 2.6. The mixing composition by weight of the mixture and the major parameters are given in Table 1.

2.2. Samples and testing programs

The cementitious materials ingredients, coarse aggregates and fine aggregates were mixed for about 1 min, and then the water was added in 1 min slowly. Finally, the ingredients were mixed for about 2–3 min. Concrete specimens were 100 mm cubes cast in steel molds and compacted by a 1 m × 1 m vibrating table. All specimens were removed from the molds 24 h after casting and then cured in a condition of 20 ± 3 °C and 95 percent RH (relative humidity) for 23 days. A portion of the specimens were then immersed in water for 4 days before being exposed to the freeze–thaw cycles.

In this paper, the freeze–thaw cycling test was performed in the freeze–thaw apparatus [17] according to GBJ82-85. The temperature of the concrete samples was controlled by a thermometer embedded in the center of the concrete specimen. In a single cycle, the temperature of the specimens cools from 6 °C to −15 °C and then warms to 6 °C all within approximately 2.5–3 h.

The mechanical tests were conducted in a special triaxial testing machine [17] (designed by State Key Laboratory of

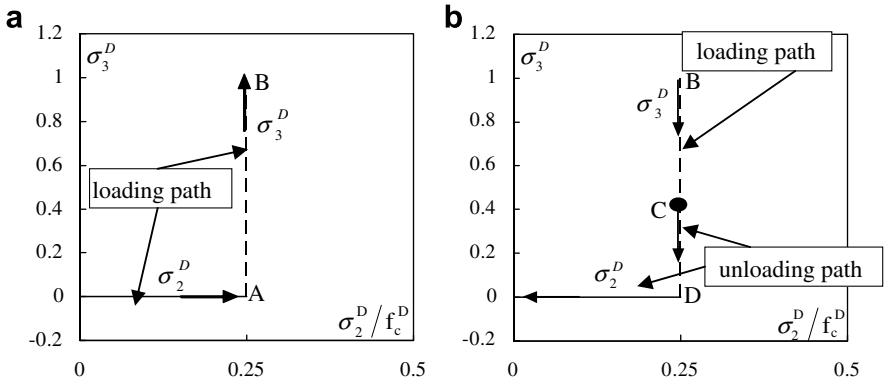

Fig. 1. The loading and unloading paths when lateral compressive stress ratio $\alpha = 0.25$.

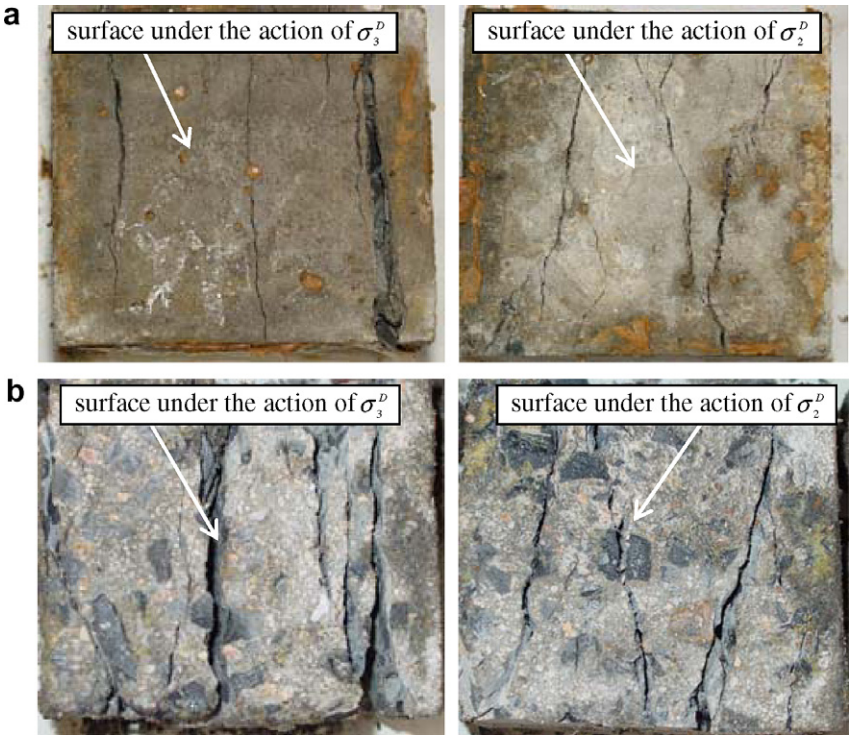

Fig. 2. The failure mode and surface cracking of specimen: (a) 0 cycles of freeze–thaw; (b) 300 cycles of freeze–thaw.

Coastal and Offshore Engineering, Dalian University of Technology) that is capable of developing three independent compressive or tensile forces. The testing of the specimens can be carried out strain-controlled, and the loading speed was 0.002 mm per second. The two load directions can be controlled together and each axis for itself. So it is possible to follow any strain path until the failure of the specimen is reached. The lateral compressive stress ratios $\alpha(\alpha = \sigma_2/f_c^D) = 0.0$ (uniaxial compression), 0.25, 0.5 and 0.75 were used. The principal stresses are expressed as $\sigma_1 \geqslant \sigma_2 \geqslant \sigma_3$ (compression denoted as positive and tension denoted as negative). Three layers of butter and three layers of plastic membrane were used as a friction-reducing [18] pad to measure the ultimate compressive strength. A minimum of three specimens was tested for each batch.

The load in the direction σ_3^D will be applied after the load σ_2^D reach the initialization (point A in Fig. 1a); and the operation should be stopped by hand after the value of load σ_3^D decrease to 40–50% of the maximum (point B is the maximum of load σ_3^D, and C is 40–50% of the maximum). The load in the direction of σ_3^D should be uninstalled firstly, and then the load σ_2^D.

σ_3^D is the maximal principal stress of air-entrained concrete under compression with lateral confined stress after freeze–thaw cycles, σ_2^D is the lateral confined compressive stress after freeze–thaw cycles, f_c^D is the uniaxial compressive strength of air-entrained concrete after freeze–thaw cycles.

3. Results and analysis σ_2^D

3.1. Failure modes

The splitting tensile strain along the unload plane(s) was the cause of failure for air-entrained concrete specimens under uniaxial compression and the compression with lateral confined stress. And it is obvious that the influence of freeze–thaw cycles on air-entrained concrete did not change the tensile splitting mode from occurring. Unlike the column-type fragments observed under uniaxial compression for air-entrained concrete after different cycles of freeze–thaw, it is plate-type and slant-shear failure under the compression with lateral stress as shown in Fig. 2a and b.

Tensile strain will result in the direction of $\sigma_1^D(\sigma_1^D = 0)$ because of the action of compressive stress σ_3^D and σ_2^D; cracking will result when the strain is larger than the ultimate tensile strain of the concrete specimen. It can be seen that the plate-type failure mode formed in the surface of σ_3^D, the slant-shear failure mode were formed in the surface of σ_2^D. The number of cracks increases as freeze–thaw cycles were increased. These studies also showed that providing a small confinement stress along the minor principal stress σ_2^D direction changed the failure modes from the common column-type to plate-type failure mode.

Fig. 3 shows SEM micro-photographs of air-entrained concrete specimen prior to freeze–thaw cycles and after 400 cycles of freeze–thaw. It can be seen from Fig. 3a that

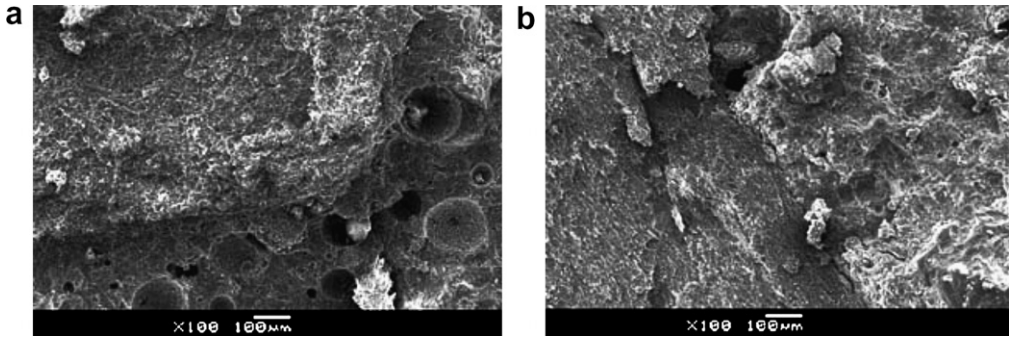

Fig. 3. SEM micro-photographs of air-entrained concrete specimen after different cycles of freeze–thaw: (a) prior to freeze–thaw cycles; (b) 400 cycles of freeze–thaw.

there is no crack between coarse aggregates and cement part as well as in cement part; the coarse aggregates did not split and the cement slurry is intact; the air bubble in the cement part is well-proportioned and intact. Fig. 3b shows the cement part becoming loose and cracking of the cement part is caused after 400 cycles of freeze–thaw; and the crack between coarse aggregates and cement part expands greatly. The coarse aggregates and cement part is separated because of the action of freeze–thaw cycles.

3.2. Experimental results

The experimental results of ultimate compressive strength of air-entrained concrete with constant confined stress are listed in Table 2. The compressive stresses σ_2^D and σ_3^D were calculated by dividing the compressive loads by the area of loading (0.01 m^2).

3.2.1. Influence of stress ratio on stress σ_3^D

It can be seen from Table 2 that the ultimate compressive strength of air-entrained concrete with constant confined stress improved greatly because of the action of lateral compressive stress after the same number of freeze–thaw cycles. The increasing percentage of ultimate compressive strength under different lateral stress compared with uniaxial compressive strength is shown in Table 3. The increasing value will change with the lateral stress ratio. The increasing percentage is largest when the stress ratio was equal to 0.5 after the same cycles of freeze–thaw, and then the value will decrease. And this is in agreement with the conclusion on non-air entrained concrete in the reference [7]. While this is disagreement with the conclusion in the reference [8] that the ultimate compressive strength of plain concrete became larger with the constant confined stress increase. Fig. 4 shows the influence of stress ratio on the increasing percentage of ultimate compressive strength under different lateral stress after different cycles of freeze–thaw compared with uniaxial compressive strength.

Besides, it can be seen from Table 3 that the increasing percentage of ultimate compressive strength compared with uniaxial compressive strength under the same lateral stress will become larger as the freeze–thaw cycles is repeated.

Table 2
Ultimate compressive strength of air-entrained concrete with constant confined stress after different cycles of freeze–thaw (MPa)

Number of freeze–thaw cycles	The compression with constant confined stress						
	0	0.25 f_c^D		0.5 f_c^D		0.75 f_c^D	
	f_c^D	σ_3^D	σ_2^D	σ_3^D	σ_2^D	σ_3^D	σ_2^D
0	26.46	31.52	6.62	33.07	13.23	31.78	19.85
100	23.96	29.93	5.99	31.86	11.98	29.47	17.97
200	21.61	27.36	5.40	29.17	10.81	26.84	16.21
300	17.53	22.86	4.38	23.98	8.77	21.58	13.15
400	13.33	18.49	3.33	19.56	6.67	17.25	10.00

Table 3
Increasing percentage of ultimate compressive strength compared with uniaxial compressive strength under different lateral stress (%)

Stress ratio $\alpha = \sigma_2^D/\sigma_3^D$	Number of freeze–thaw cycles								
	Test data in this paper					Test data in Ref. [8]			
	0	100	200	300	400	0	25	50	75
0.25 f_c^D	19.12	24.92	26.61	30.41	38.71	16.7	26.7	37.8	42.2
0.5 f_c^D	24.98	32.97	34.98	36.79	46.74	22.1	34.1	51.3	55.0
0.75 f_c^D	20.11	23.0	24.20	23.10	29.41	39.3	50.3	62.0	63.9

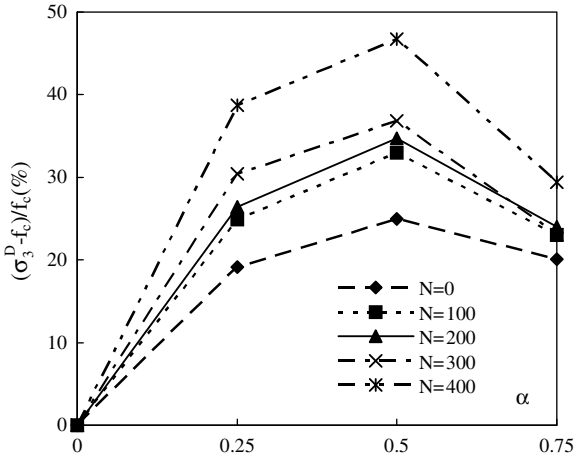

Fig. 4. Influence of stress ratios α on stress σ_3^D.

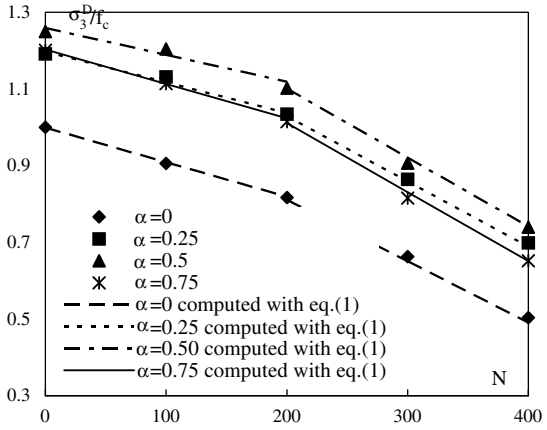

Fig. 5. Compressive strength versus number of freeze–thaw under different lateral stress ratios α.

When the lateral compressive stress ratio was equal to 0.5, the ultimate compressive strength was about 1.25 times the uniaxial compressive strength prior to freeze–thaw cycles; while the ultimate compressive strength increased to about 1.47 times the uniaxial compressive strength after 400 cycles of freeze–thaw. The finding is agreement with the conclusion got by Qin [8]. The ultimate compressive strength with constant confined stress is about 1.22 times the uniaxial compressive strength for plain concrete prior to cycles of freeze–thaw, while it was 1.55 times the uniaxial compressive strength after 50 cycles of freeze–thaw in the reference [8]. The ultimate compressive strength of air-entrained concrete with constant confined stress varied from 1.19 to 1.25 times the uniaxial compressive strength at the different stress ratios prior to freeze–thaw cycles; however, it varied from about 1.23 to 1.35 at different stress ratios after 300 cycles of freeze–thaw.

3.2.2. Influence of freeze–thaw cycles on stress σ_3^D

Table 4 gives the decreasing percentage of ultimate compressive strength of air-entrained concrete under different lateral stress as number of freeze–thaw cycles increased. It was apparent that the decreased percentage is larger for specimens under uniaxial compression than under compression with constant confined stress; and the strength loss will become lager as the freeze–thaw cycles increased. The relationship between ultimate compressive strength and number of freeze–thaw cycles is shown in Fig. 5. It can be seen from Table 4 and Fig. 5 that the freeze–thaw cycles had less effect on the strength of air-entrained concrete during the initial 200 freeze–thaw cycles compared to after the initial 200 freeze–thaw cycles. It can be also seen from Fig. 5 that σ_3^D/f_c is largest when the lateral stress ratio $\alpha = 0.5$.

Table 4
Loss of ultimate compressive strength σ_3^D under different lateral stress with increasing of freeze–thaw cycles (%)

Number of freeze–thaw cycles	Constant confined stress			
	0	0.25 f_c^D	0.5 f_c^D	0.75 f_c^D
100	9.45	5.04	3.66	7.27
200	18.33	13.20	11.79	15.54
300	33.75	27.47	27.49	32.10
400	49.62	41.34	40.85	45.72

3.3. Discussion

Concrete is a three-phase composite material at microscopic scale: a cement part, aggregate and the interfacial transition zone between the two. The microcracks will be formed due to drying and thermal shrinkage mismatch of aggregate particles and the cement part. Below the freezing point of water in microcracks, the volume increase of ice causes tension in the surrounding concrete which depending on the degree of saturation and type of material and structure etc. If the tensile stress exceeds the tensile strength of concrete, microcracks occur. By continuing freeze–thaw cycles, more water can penetrate the existing cracks during thawing, causing higher expansion and more cracks during freezing just Fig. 3 shows. On the other hand, considering the concrete specimen under compression with constant confined stress, the initiation and growth of every new crack will reduce the load carrying area. This reduction in load carrying area further causes an increase in the stress concentration at critical crack tips. So the compressive strength of plain concrete under compression with constant confined stress decreased with repeated freeze–thaw cycles.

Air-entrained concrete contains a very high number of microscopic air bubbles when air-entraining agents are used. These relieve internal pressure on the concrete by providing tiny chambers for the expansion of water or growth of ice during freezing which depending on the degree of saturation. So after the same cycles of freeze–thaw, the strength loss of air-entrained concrete is lower than that of plain concrete.

Table 5
Regressive coefficient a, b and correlative coefficient r

Lateral stress ratio α	$0 \leqslant N \leqslant 200$				$200 \leqslant N \leqslant 400$			
	0	0.25 f_c^D	0.5 f_c^D	0.75 f_c^D	0	0.25 f_c^D	0.5 f_c^D	0.75 f_c^D
a	0.9991	1.1974	1.2591	1.2031	1.1304	1.3684	1.4608	1.3709
b	−0.0009	−0.0008	−0.0007	−0.0009	−0.0016	−0.0017	−0.0018	−0.0018
r	1.0	0.9818	0.9542	0.9986	1.0	1.0	0.9979	0.9969

4. Failure criteria

4.1. Relationship between stress σ_3^D and freeze–thaw cycles

The relation between stress σ_3^D and the number of freeze–thaw cycles can be expressed as follows:

$$\frac{\sigma_3^D}{f_c} = a + b * N, \tag{1}$$

where f_c is the uniaxial compressive strength of air-entrained concrete prior to freeze–thaw cycles, N is the number of freeze–thaw cycles; a and b is the regression coefficient. Table 5 gives the regression coefficients and the correlation coefficient r from simple linear regression using the test data.

Fig. 5 illustrates the comparison of the calculated results obtained from formula (1) and the test results. It can be seen that they are in good agreement.

4.2. Relationship between stress σ_3^D and lateral compressive stress ratio

The relationship between stress σ_3^D and lateral stress ratio under the compression with constant confined stress after different cycles of freeze–thaw can be expressed as follows:

$$\frac{\sigma_3^D}{f_c} = \frac{c + d\frac{\sigma_2^D}{f_c^D}}{\left(1 + \frac{\sigma_2^D}{f_c^D}\right)^2}, \tag{2}$$

Table 6
Computed value σ_3^D/f_c after different cycles of freeze–thaw

Lateral stress	Number of freeze–thaw cycles				
	0	100	200	300	400
0	26.20	24.60	22.35	18.74	14.72
0.25 f_c^D	31.98	30.06	27.40	22.48	17.97
0.5 f_c^D	32.78	30.82	28.12	22.90	18.42
0.75 f_c^D	31.84	29.95	27.35	22.17	17.90

where c, d are the regression coefficients; $a = 0.9901$, 0.9296, 0.8447, 0.7081, 0.5564; $b = 3.5942$, 3.3831, 3.0937, 2.4779, 2.0199 respectively and correlation coefficient $r = 1.0$, 0.9968, 0.996, 0.9918, 0.9856, respectively, is defined from multiple linear regression using the test results after 0, 100, 200, 300, 400 cycles of freeze–thaw. Table 6 gives the computed value of air-entrained concrete under lateral stress after different freeze–thaw cycles according to the formula (2).

4.3. The unified failure criterion relating to the influence of freeze–thaw cycles and stress ratio

The failure criterion is proposed as follows:

$$\frac{\sigma_3^D}{f_c} = \left[a_1 + a_2 N + \frac{a_3\alpha + a_4}{(1+\alpha)^2}\right] \tag{3}$$

in which α is the lateral compressive stress ratio; a_1, a_2, a_3 and a_4 are the regression coefficients. $a_1 = -0.1805$,

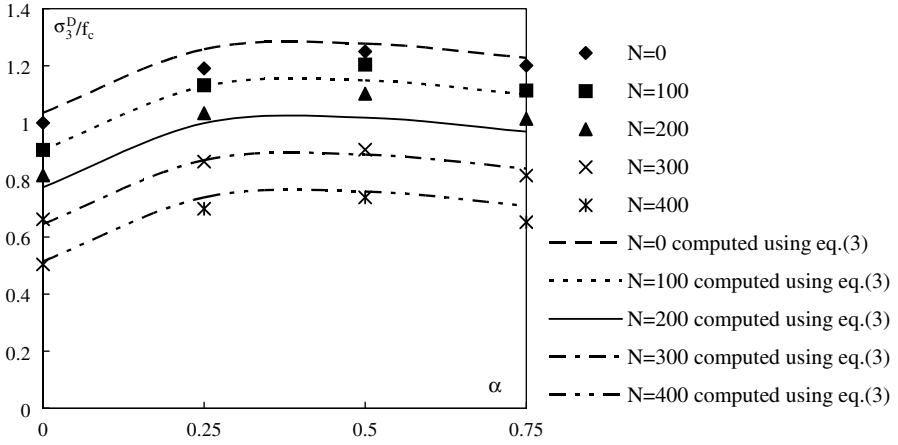

Fig. 6. Comparison between the computed value by the unified failure criterion and experimental results.

$a_2 = -0.0013$, $a_3 = 4.1356$,$a_4 = 1.2151$ and correlative coefficient $r = 0.9672$ can be obtained though multiple linear regression using the test data.

A comparison of the calculated data obtained from Eq. (3) with experimental data is shown in Fig. 6.

5. Conclusion

Based on the experimental work and the analysis of the test results, the following conclusions can be drawn:

1. The failure mode of air-entrained concrete did not change after different cycles of freeze–thaw;
2. the ultimate compressive strength with constant confined stress is greater than the uniaxial compressive strength at all stress ratios after the same cycles of freeze–thaw. The strength increase depends on the lateral compressive stress ratio;
3. the relationship between stress σ_3^D, number of freeze–thaw cycles and the lateral stress ratio is given and a unified failure criterion relating to the number of freeze–thaw cycles and stress ratio is proposed;
4. the experimental results and analysis model will help enable more broad application, sound structural design and maintenance by taking into consideration the freeze–thaw durability of air-entrained concrete under the compressive loads with constant confined stress.

References

[1] Mather Bryant. Concrete durability. Cement Concrete Comp 2004;26:3–4.
[2] Parviz Soroushian, Mohamad Nagi, Austin Okwuegbu. Freeze–thaw durability of lightweight carbon fiber reinforced cement composites. ACI Mater J 1992;September–October:491–4.
[3] Alexander MG, Magee BJ. Durability performance of concrete containing condensed silica fume. Cement Concrete Res 1999;29:917–22.
[4] Jacobsen Stefan, Sellevold Eirk J, Matala Seppo. Frost durability of high strength concrete: the effect of internal cracking on ice formation. Cement Concrete Res 1996;66(6):919–31.
[5] Buck AD. Recycled concrete as a source of aggregate. ACI Mater J 1977;74(5):212–9.
[6] Sun W, Zhang YM, Yan HD, Mu R. Damage and damage resistance of high strength concrete under the action of load and freeze–thaw cycles. Cement Concrete Res 1999;29:1519–23.
[7] Shang HS, Song YP. Experimental study of strength and deformation of plain concrete under biaxial compression after freezing and thawing cycles. Cement Concrete Res 2006;36:1857–64.
[8] Qin Li-Kun, Study on the strength and deformation of concrete under multiaxial stress after high-temperature of freeze–thaw cycling, Dalian University of Technology. Doctoral dissertation, 2003.
[9] Kupfer H, Hilsdorf HK, Rusch H. Behavior of concrete under biaxial stresses. J ACI 1969;66(8):656–66.
[10] Torrenti JM. Behavior of steel-fibre-reinforced concrete under biaxial compression loads. Cement Concrete Comp 1995;17:261–6.
[11] Traina LA, Mansour SA. Biaxial strength and deformational behavior of plain and steel fiber concrete. ACI Mater J 1991;88(4).
[12] Lee SK, Song YC, Han SH. Biaxial behavior of plain concrete of nuclear containment building. Nucl Eng Des 2004;227:143–53.
[13] Lan Sheng-Rui, Guo Zhen-Hai. Experimental investigation of deformation characteristics of concrete under biaxial compression with constant confined stress. China Civil Eng J 1996;29(2):28–36.
[14] Lü Pei-yin, Song Yu-pu, Wu Zhi-min. Strength and deformation characteristics of concrete subjected to different loading rates combined with confined stress. J Dalian Univ Technol 2001;41(6):716–20.
[15] Lü Pei-yin, Song Yu-pu, Hou Jing-Peng. Experimental study and failure criterion of compression concrete under various loading rates with uniaxial lateral confinement. Eng Mech 2002;19(5):67–71.
[16] GBJ82-85. The test method of long-term and durability on ordinary concrete. National Standard of the People's Republic of China; 1997.
[17] Li-kun Qin, Yu-pu Song, Yu-jie Wang, Yu Chang-jiang, Zhang Zhong. The influence of cycles of freezing and thawing on the compressive property of concrete in seawater. Concrete 2004:16–8.
[18] Lü Pei-yin, Song Yu-pu. Dynamic compressive test of concrete and its constitutive model. Ocean Eng 2002;20(2):43–8.